

Phase-slip mechanism for dissipation in high- T_c superconductors

A. C. Wright, T. K. Xia, and A. Erbil*

School of Physics, Georgia Institute of Technology, Atlanta, Georgia 30332

(Received 27 June 1991; revised manuscript received 15 October 1991)

The phase-slip theory of Ambegaokar and Halperin (AH) is used to explain measurements of magnetoresistance versus temperature for a granular high- T_c superconducting material, assuming an array of Josephson weak links. Results of experiments are compared to dynamical calculations of the critical current versus magnetic field in a Josephson-junction array at non-zero temperatures. The AH theory is able to account for the observed dissipation, give physical insight into the role played by the sample microstructure, and also quantitatively explain the kink in the magnetoresistance curve seen to occur in both granular and single-crystal materials. Furthermore, within this framework, the critical current for a particular sample is determined from magnetoresistance measurements, and then used to calculate the temperature dependence of the ac magnetic susceptibility. Comparison of the calculated real and imaginary components is made to direct measurements.

I. INTRODUCTION

Understanding of the dissipation mechanism in high- T_c superconductors is extremely important for its scientific and technological implications. Whether all of the seemingly different types of dissipation mechanisms in superconductors can be explained by using a single formalism remains to be seen. Tinkham¹ demonstrated semiquantitatively the plausibility of equating thermally activated flux motion with the 2π phase-slip dynamics of a single Josephson junction, as worked out by Ambegaokar and Halperin² (AH) for a heavily damped, current-driven junction. In a previous paper,³ we extended the ideas of Tinkham by pointing out that in AH theory, the phase-slip barrier is proportional to the critical current of the junction, and, when applied to an array of Josephson weak links, the field dependence of the phase-slip barrier can be modeled by a suitable averaging of the junction parameters.

In this paper, we present further evidence supporting the applicability of AH theory to dissipation in high- T_c superconductors and its potential usefulness as a conceptual framework for any superconductor. That is, arrays of coupled Josephson junctions may serve as a model not only for weakly coupled grains, but also for a continuum or "single-crystal" material, corresponding to the limit of strongly interacting grains. Since the AH equations are derived for a single junction, their success in describing a network of Josephson junctions supports an effective-medium picture, as described by Tinkham and Lobb.⁴

The format of the paper is as follows: In Sec. II we review the results found in Ref. 3 for fitting R - T and I - V data to AH equations, and present magnetoresistance data which, when fitted to AH expressions, yield further insights. Dynamical calculations of the critical current of an array of Josephson junctions under different magnetic-field values at different temperatures are also shown; in Sec. III the field and temperature dependences of the phase-slip barrier energy and its relationship to the

measured critical current are discussed. Furthermore, the usefulness of AH theory for explaining the kink in the resistivity curve seen in both granular and single-crystal materials is demonstrated. Finally, within the context of AH theory, the ac magnetic susceptibility is calculated by using a critical-state model which is unique to the sample's microstructure. This is then compared to ac susceptibility measurements on our samples. Section IV gives our summary and conclusions. Experimental details were given in Ref. 3. Sample preparation and characterization are planned to be presented elsewhere.

II. RESULTS

A. Magnetoresistance data

Results of measurements of resistance versus temperature in various applied magnetic fields were shown in Ref. 3, fitted to the small current limit of AH theory,² namely,

$$R = R_n [I_0(\frac{1}{2}\gamma)]^{-2}, \quad (1)$$

where R_n is the normal resistance of the Josephson junction, I_0 is the modified Bessel function, and $\gamma = \hbar I_1 / ek_B T$, with I_1 the maximum supercurrent of the junction in the absence of thermal fluctuations. γ is the normalized barrier height of the sinusoidal potential encountered by the phase difference as it evolves in time. We can assume $\gamma = U_0 / k_B T$, where U_0 is the activation energy for the phase slip. I_1 was chosen to have an explicit temperature dependence, but an unspecified field dependence, given by $I_1 = A(H)(1-t)^m$, where $t = T/T_c$ and $m = \frac{3}{2}$. Thus, $\gamma = A'(H)(1-t)^{3/2}$ for T near T_c .¹ The fits are shown in Fig. 1 of Ref. 3 for which A' , R_n , and T_c were varied as parameters. As can be seen in Fig. 1 of Ref. 3, Eq. (1) has in it the qualitative behavior of both the "flux creep" and "flux flow" regimes. The flux creep regime is the exponential-like curvature at near-zero resistances, while the flux flow regime is seen at resistances near the onset of the field-induced broadening.

Since γ , the normalized energy barrier, is proportional to the Josephson critical current in AH theory, one would expect the field dependence of γ to vary as a Fraunhofer diffraction function. This expectation is justified since λ_J , the Josephson penetration distance, is much larger than the typical grain-boundary junction dimension at all temperatures.⁵ However, for granular material, in which an array of Josephson weak links exists, one must average the Fraunhofer function over the sizes of the junctions and their orientations relative to the applied field.⁶ Thus, in Ref. 3, γ versus magnetic field was extracted from R - T data and fitted to such an averaged Fraunhofer function, given by

$$\frac{\gamma(H)}{\gamma(H=0)} = C \int_0^\infty p(x) dx \int_{\theta}^{\pi/2} \left| \frac{\sin(xy \sin\theta)}{xy \sin\theta} \right| d\theta + \gamma_0, \quad (2)$$

where $p(x)$ is a log-normal distribution (of junction sizes) and C is a constant. $x = L/L_m$ is the junction length normalized to a mean length L_m and $y = H/H_0$ is the applied field, normalized to a quasiperiod $H_0 = \Phi_0/\mu d L_m$ with Φ_0 the flux quantum and d the mean junction thickness perpendicular to the field. γ_0 is a field-independent constant. d is actually an effective thickness, equal to $2\lambda + \delta$, where λ is the Ginzburg-Landau penetration depth and δ is the thickness of the barrier layer.

Also in Ref. 3, voltage versus current at various temperatures in zero applied field was measured and fitted to the simplified analytic AH expression.² γ versus temperature was then extracted from these data, yet the correct power-law exponent of the temperature dependence was ambiguous. A further investigation of the correct temperature dependence of γ is possible, however, by measuring the resistance as a function of applied magnetic field for various temperatures. Such data are presented here in Fig. 1(a). For these measurements, a dc current of 0.43 mA was applied perpendicular to the external magnetic field. This was the smallest current we were able to use and still obtain good signal-to-noise ratio. A small transport current is desirable in order to approximate the conditions for which Eq. (1) holds. The solid lines in Fig. 1(a) are fits to Eq. (1), but with $\gamma = A_1(H^2 + A_2)^{-1} + A_3$. In this way, the averaged Fraunhofer field dependence of γ was approximated for computational convenience by a Lorentzian line shape plus a constant offset, thus retaining the characteristic zero slope and rounding at zero field. We in fact attempted other similar forms, including a Gaussian and a hyperbolic secant, yet the Lorentzian produced the best fit to $\gamma(H)$. For each temperature, A_1 , A_2 , and A_3 were varied while R_n was held constant at 10 m Ω , the same value used in fitting to R - T and I - V data.

The results from fitting to Eq. (1) at each temperature are plotted in Fig. 1(b) as γ versus magnetic field. They exhibit a trend similar to that typically reported for measured critical currents as a function of magnetic field at nonzero temperatures.⁷ It should be noted that the parameters A_1 , A_2 , and A_3 , corresponding to the amplitude, width, and zero offset, respectively, of each

Lorentzian, have some temperature dependence, as can be seen in Fig. 1(b). Though the fitted values of the parameters are in the expected range, the curves in Fig. 1(b) suggest that γ does not scale with a simple $(1-t)^m$ factor. This nonscaling behavior is expected for a single Josephson junction, since the penetration depth changes with temperature.⁸ We will show in the next section that this behavior is also expected for a coupled Josephson-junction array.

B. Dynamical calculation of critical current

The γ - H curves at various temperatures shown in Fig. 1(b) are for a granular high- T_c superconductor, which can be modeled as an ensemble of weakly coupled superconducting grains. The explanation of the behavior of

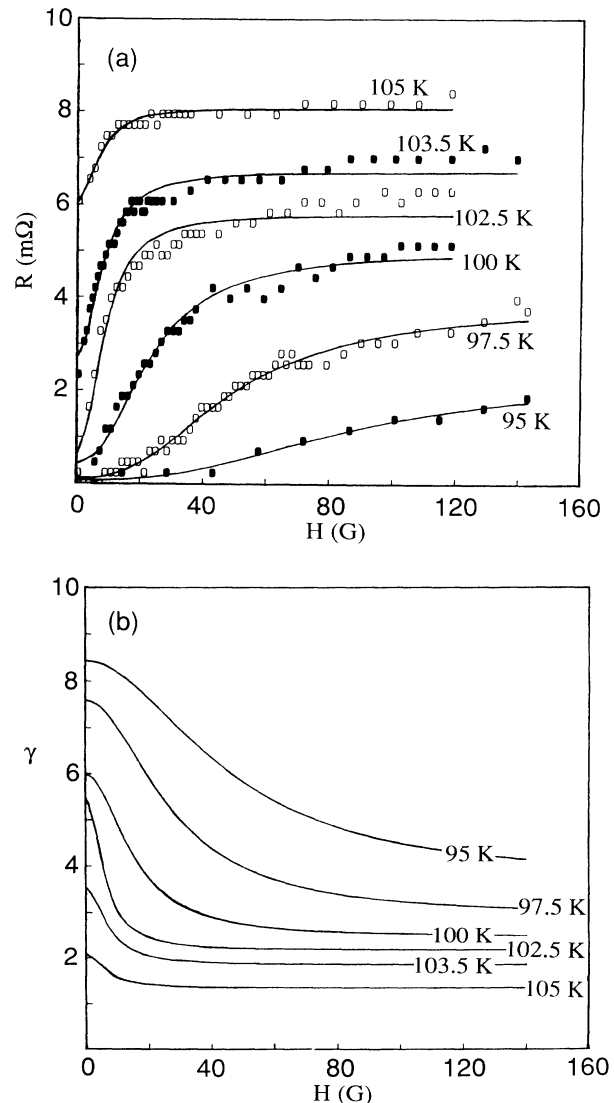


FIG. 1. (a) Resistance vs magnetic field at various temperatures, fitted (solid lines) by using Eq. (1) with $\gamma = A_1(H^2 + A_2)^{-1} + A_3$. (b) γ vs magnetic field obtained from the fittings shown in (a) for various temperatures.

these curves therefore requires one to consider the dynamical effect of thermally fluctuating currents, especially when T is close to T_c , on a Josephson-junction array rather than on a single junction. Thus we go beyond the AH model to calculate the critical current of a superconducting array as a function of temperature in the presence of magnetic field.

Two-dimensional arrays of Josephson junctions have been studied numerically by solving a set of coupled differential equations representing the dynamics of the junctions. These have been studied as functions of temperature, and also of the applied magnetic field or the frustration. The frustration is defined as the magnetic flux per plaquette of the junction array, normalized to the flux quantum: $f = sH/\Phi_0$, where s is the area of a plaquette and H is the applied field perpendicular to the array. We use the method of Falò, Bishop, and Lomdahl to solve a set of coupled nonlinear differential equations.^{9(a)} The time dependence appears in the phases ϕ_i of the order parameters of N superconducting grains. These grains are Josephson coupled and resistively as well as capacitively shunted. The N coupled differential equations are given by^{9(b)}

$$I_i^{\text{ext}} = \sum_j \left[\frac{\hbar}{2e} C_{ij} \frac{d^2}{dt^2} (\phi_i - \phi_j) + \frac{\hbar}{2eR_{ij}} \frac{d}{dt} (\phi_i - \phi_j) + I_{c;ij} \sin(\phi_i - \phi_j - A_{ij}) \right]. \quad (3)$$

In this expression, t is time; $I_{c;ij}$ is the junction critical current between grains i and j ; I_i^{ext} is the external current fed into grain i ; C_{ij} is the coupling capacitance between grains i and j while C_{ii} is the capacitance of grain i to the ground; R_{ij} is the shunt resistance between grains i and j ; and A_{ij} is the gauge-invariant phase factor

$$A_{ij} = \frac{2\pi}{\Phi_0} \int_{x_i}^{x_j} \mathbf{A} \cdot d\mathbf{l},$$

where x_i is the center of grain i and \mathbf{A} is the vector potential. The A_{ij} obey the constraint that the sum around any unit cell of the array is constant

$$A_{ij} + A_{jk} + A_{kl} + A_{li} = 2\pi f,$$

where f is the frustration defined above. The voltage drop across the junction is related to the phase difference by the Josephson relation

$$\frac{d}{dt} (\phi_i - \phi_j) = \frac{2e}{\hbar} (V_i - V_j).$$

Equation (3) can be rewritten for computational convenience by defining a reduced time $\tau = t/t_0$, with $t_0 = \hbar/2eR_{ij}I_{c;ij}$, as follows:

$$\frac{I_i^{\text{ext}}}{I_{c0}} = \sum_j \left[\beta C_{ij} \frac{d^2}{d\tau^2} (\phi_i - \phi_j) + \frac{d}{d\tau} (\phi_i - \phi_j) + \sin(\phi_i - \phi_j - A_{ij}) \right],$$

where $\beta = 2eR_0^2 I_{c0}/\hbar$. Here, $I_{c;ij}$ and R_{ij} are set equal to

I_{c0} and R_0 , according to the assumption of identical junctions with nearest-neighbor interaction only.

For nonzero temperatures, we assume a fluctuating noise current in each shunt resistance, similar to that assumed by AH. The noise currents in the shunt resistances of different junctions are uncorrelated. These equations thus can be viewed as a generalization of the AH single-junction model.^{9(b)} Furthermore, in the overdamped limit ($C_{ij} \rightarrow 0$), they describe the extensively studied resistively shunted junction (RSJ) model of a resistively shunted Josephson-junction array.^{9(c)} The numerical solution of Eq. (3) directly yields the I - V curve, from which the macroscopic critical current can be obtained as the point at which a certain jump in the voltage occurs. Chung, Lee, and Stroud solved the RSJ equations of motion at zero temperature for various array sizes and values of frustration and plotted the critical current as a function of frustration values.^{9(c)} The data resemble averaged Fraunhofer functions with magnetic field. We extended these calculations to nonzero temperatures, choosing a $L_x \times L_y$ array with $L_x = 11$ and $L_y = 10$. In the simulations, we used periodic boundary conditions in the y direction and free boundary conditions in the x direction, where the x direction is that of the external current. The overdamped limit was assumed by taking $\beta C_{ii} = 0.04$ and $\beta C_{ij} = 0$. The details of the calculating algorithm can be found in Ref. 9(b).

Figure 2 shows the calculated reduced critical current I_c/I_{c0} , where I_{c0} is the critical current at zero field, plotted as a function of frustration for three different reduced temperatures T^* , where $T^* = ek_B T/\hbar I_{c0}$. $T^* = 0, 0.05$, and 0.5 corresponds to 0 K, 94.6 K, and 107.7 K, respectively, if we assume $m = \frac{3}{2}$, as used in fitting our R - T data. The magnetic-field dependence in Fig. 2 is qualitatively similar to that shown in Fig. 1(b). We note that for the $T^* = 0$ case in Fig. 2, significant falloff of the critical current already occurs at a frustration value $f = 0.05$. In real granular superconductors, as in the samples we used, superconducting loops or arrays certainly would have a distribution of areas and orientations, as well as a variety of topological shapes. A more detailed comparison with experiment hence would require averaging over these quantities.

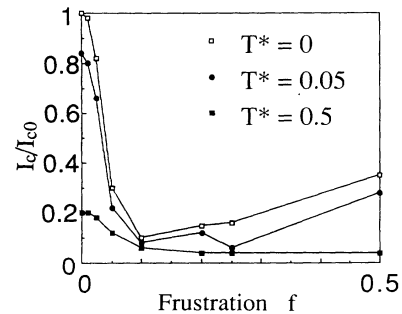


FIG. 2. Calculated reduced critical current (I_c/I_{c0}) as a function of frustration f at various reduced temperatures T^* for a 11×10 Josephson-junction array. The calculations are done in the overdamped limit with $\beta C_{ii} = 0.04$ and $\beta C_{ij} = 0$, where $\beta = (2eR_0^2 I_{c0}/\hbar)$.

III. DISCUSSION

A. Interference effects

As mentioned in Sec. II A above, we modeled the field dependence of γ as a Fraunhofer function which was averaged over the size distribution of the Josephson weak links connecting the grains of the material [Eq. (2)]. The Fraunhofer interference function is known to arise in a single junction due to the spatial dependence of the phase difference ϕ along the length of the junction, analogous to the single slit diffraction of light. Yet a spatially dependent phase difference can also be defined for an array of junctions in a magnetic field, as was done in Sec. II B. In that case, a gradient in the phase difference existed over the length of the array, so that the individual junction phase differences interfered as in a single slit. The calculated field dependence of the critical current thus displayed a smooth, Fraunhofer-like behavior similar to Eq. (2). However, the smoothing effect is inherent to this calculation, which is for an array of identical junctions, rather than arising from averaging over a distribution of junction sizes.

Another phenomenon which has been shown to smooth out the Fraunhofer pattern of single junctions is the existence of fluctuations in the thickness of the junction barrier layer.⁸ The results of Secs. II A and II B above therefore suggest a model for our granular material as an effective junction, with effective structural disorder in the barrier layer corresponding to the junction array.

B. Measured critical current and I_1

A few words should be said about the relationship between the measured critical current I^{meas} , defined with a voltage criterion, and the junction critical current I_1 , to which γ is proportional. I_1 and I^{meas} have clearly different field dependences. We measured the field dependence at 98 K of the macroscopic critical current I^{meas} , which is the applied transport current at which the measured voltage drop is $0.5 \mu\text{V}$. The data resemble a smoothed Fraunhofer function and decay asymptotically to zero. In a manner identical to that of Peterson and Ekin,⁶ we were then able to fit these data to Eq. (2) without the need of an added constant γ_0 . In doing so, the same value of the quasiperiod H_0 was obtained as from the fitting to I_1 vs H in Fig. 2 of Ref. 3, which may be expected from a common microstructure. However, this field dependence is different from that of the parameter I_1 , which was found to resemble a smoothed Fraunhofer function decaying to a nonzero asymptote (γ_0).

It has been demonstrated⁸ for a single Josephson junction that both thermal fluctuations and structural fluctuations within the barrier have a smoothing effect on the Fraunhofer interference function of the critical current versus field. The difference between these two effects is seen most clearly at higher fields, at which the former quenches superconductivity, while the latter leads to a nonzero, field-independent supercurrent. This is consistent with what we observe, since I_1 is free from

thermal fluctuations, whereas I^{meas} includes the smearing due to thermal phase slippage.

We conclude that I_1 rather than I^{meas} is the correct quantity to fit to a Fraunhofer function that is averaged over junction sizes. However, the measured I^{meas} can be used to calculate I_1 via the AH full integral expression,² thus removing the thermal fluctuation effects. For instance, Dubson *et al.*¹⁰ point out the similarity of I_1 versus field, when averaged over ten junctions of different sizes, to the field dependence of the temperature “ T_c ,” at which the sample voltage falls below 5 nV with a sample current of 1 mA. This “ T_c ” could be converted into I_1 by employing the AH integral relation for a proper comparison.

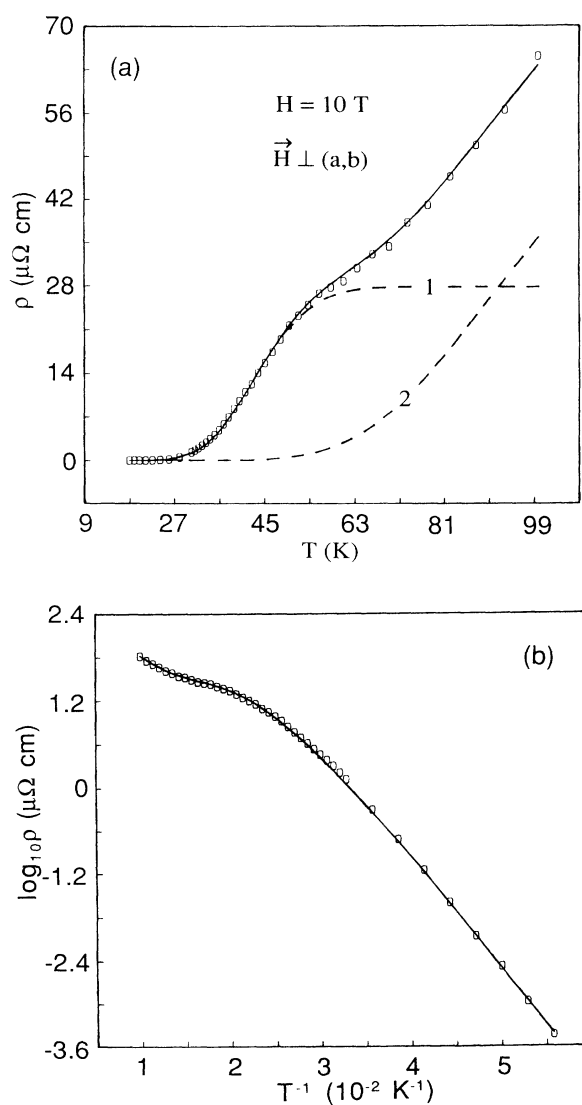


FIG. 3. Resistivity vs temperatures in a 10-T applied magnetic field, showing the kink (circles show the data from Ref. 11). (a) Fit to Eq. (4) shown in linear scale (solid line); also shown separately are the two contributions in Eq. (4) (dashed lines). (b) Fit to Eq. (4) shown in Arrhenius plot to emphasize the flux creep regime.

C. Magnetoresistance kink

Next, we show that the phase-slip picture developed above can explain the dissipation observed in single-crystal superconductors. Figure 3 (circles) shows the resistivity-temperature data of Palstra *et al.*,¹¹ for a $\text{Bi}_{2.2}\text{Sr}_2\text{Ca}_{0.8}\text{Cu}_2\text{O}_{8-d}$ single crystal in a field of 10 T, just below the transition onset. This data is representative of a kink often seen in high fields in both granular and single-crystal high- T_c compounds. The shape of the magnetoresistance kink has been shown to be directly related to various sample properties, such as oxygen occupancy,¹² impurity concentration,¹³ crystalline anisotropy,¹⁴ and the particular rare-earth substitution used.¹⁵ This behavior can be understood using a variation of the AH Eq. (1), given by

$$\rho = \rho_{n1} [I_0(\frac{1}{2}\gamma_1)]^{-2} + \rho_{n2} [I_0(\frac{1}{2}\gamma_2)]^{-2}, \quad (4)$$

where $\gamma_i = A_i'(H)(1 - T/T_{ci})^{3/2}/T$. Figure 3 shows the data of Palstra *et al.* fitted to Eq. (4) (solid line), on a linear scale [Fig. 3(a)] and in an Arrhenius plot [Fig. 3(b)]. As can be seen, the fit to the experimental data is remarkably good. Figure 3(a) also shows the contributions of the two terms in Eq. (4) separately (dashed lines).

The fitting gave values for ρ_{n1} and ρ_{n2} equal to the resistivities at the onset of each step, and for T_{c1} and T_{c2} somewhat greater than the visible onset temperatures of each transition step. The fitted values of γ_1 and γ_2 , if associated with junction critical currents, correspond to zero-temperature critical currents (I_1) of 8.6 μA and 13.0 μA , respectively, in a 10-T applied field. The junctions with the stronger coupling (larger I_1) are related to the upper resistivity step, which, in experiments, generally exhibits less field-induced broadening than the lower step. The coupling energy of a junction is inversely related to the amount of flux threading its area and thus also to the length and the thickness of the junction. The success of Eq. (4) therefore suggests an interpretation of the kink as the superposition of dissipative voltage contributions from junctions of two separate mean sizes within the material. Each type of junction would be averaged over its own distribution of sizes and orientations and thus have a unique field dependence of its phase-slip energy $\gamma(H)$, characterized by the rate of falloff in applied field (H_0).

In fitting, the temperature dependence used for γ_1 and γ_2 in Eq. (4) differed slightly from that used for γ in Eq. (1). Our R - T data were fitted with the approximation $1/T \approx 1/T_c$, for T close to T_c . However, the use of the $1/T$ factor was found necessary in order to fit the low levels of ρ ($< 1\% \rho_n$) in Fig. 3(b), where linear Arrhenius behavior dominates ($U_0 \gg k_B T$). This regime is commonly termed the flux creep regime, but can be fitted with the AH expression just as well as the upper level ρ ($> 1\% \rho_n$) near T_c in Fig. 3(a), which is usually distinguished as the flux flow regime. Reports that show thermally activated magnetoresistance at low temperatures^{11,14} are therefore consistent with the AH theory.

D. ac susceptibility and the critical state

The screening currents induced by an applied magnetic field can be assumed to be initially above the critical level, followed by flux motion until the Lorentz force just equals the pinning force. After such transients, the magnetic flux penetrating a sample is in a stable configuration at each value of applied magnetic field, and the flux density gradient is uniquely determined by the pinning force density in the microstructure. This field gradient is proportional to the critical current, in the limit that $B \propto H$ inside the material. Thus, an experimentally determined, nonanalytic critical-state model would be possible by measuring the critical current as a function of the applied field. Such data could be used in a numerical solution of the critical-state equation to obtain the flux density

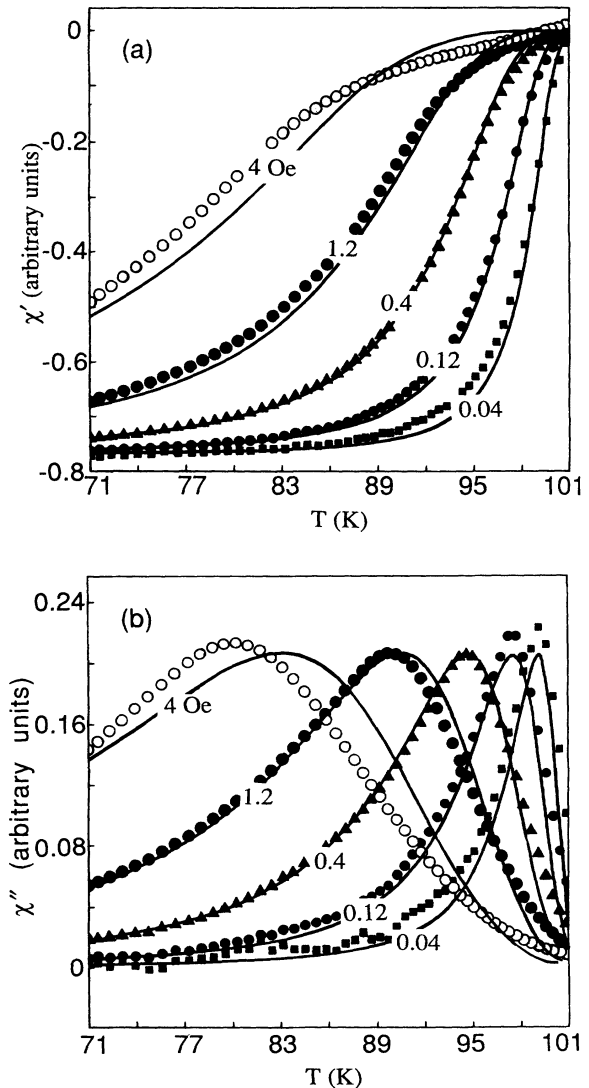


FIG. 4. Complex ac susceptibility vs temperature for various peak-to-peak values of applied ac magnetic fields at 4 kHz. Solid lines are calculated using Eqs. (5) and (6). (a) Real part $\chi'(T)$. (b) Imaginary part $\chi''(T)$.

profile interior to the sample, and ultimately in the calculation of susceptibility versus temperature $\chi(T)$. Although this solution would be nonanalytic, it would nevertheless be an exact solution for the sample.¹⁶ The $\gamma(H)$ data of Fig. 2, Ref. 3, can be used for this purpose, since they represent the field dependence of the critical current without thermal fluctuations, averaged over the microstructure of the sample. Of course, an analytic approximation to the averaged Fraunhofer function can be used also.

An explicit derivation of $\chi(T)$ from the critical-state equation has been published by Müller¹⁷ for a granular high- T_c superconductor, and also by Sun *et al.*¹⁸ for a thin film. Müller¹⁷ found good agreement with experimental $\chi(T)$ data by assuming a Kim-type critical state for the intergranular contribution and a Bean-type model for the flux density profiles within the grains. Such an assumption is in agreement with the results we obtained from fitting $\gamma(H)$ by means of a smoothed-out Fraunhofer function plus a constant. The constant term would correspond to a Bean-type contribution, in which

$$m(t) = \begin{cases} m_0 \left[\left[\frac{1}{2} + \eta \right] - \exp \left[-\frac{H_{ac}}{H^*} (1 - \sin \omega t) \right] \right], & (\pi/2 \leq \omega t \leq 3\pi/2) \\ m_0 \left[\exp \left[-\frac{H_{ac}}{H^*} (1 + \sin \omega t) \right] - \left[\frac{1}{2} + \eta \right] \right], & (-\pi/2 \leq \omega t \leq \pi/2) \end{cases} \quad (5)$$

Here, $m_0 = 2\pi J_c l a^3 / 3c$, $\eta = \frac{1}{2} \exp(-2H_{ac}/H^*)$, and $H^* = 4\pi J_c l / 3c$ is the field at which the critical state has penetrated to the center of the sample. l is the thickness and a is the radius of the sample, and J_c is the critical-current density. The ac voltage induced in the pickup coil is proportional to the time rate of change of $m(t)$. The real and imaginary parts of the susceptibility are then calculated from the first Fourier components of this ac signal.

The field and temperature dependences of J_c can be input into Eq. (5) as either fitted analytic functions or as a set of points. For the calculated curves in Fig. 4, we used a field dependence obtained by fitting the $\gamma(H)$ in Fig. 2, Ref. 3, to a Lorentzian, as follows:

$$J_c = J_{c0} \left[0.714 \left[\frac{H^2}{46.8} + 1 \right]^{-1} + 0.273 \right] (1 - T/T_c)^{2.38}. \quad (6)$$

The solid lines in Fig. 4 were made by first determining the best fit values of H^* and m_0 for the 0.4-Oe χ'' data, and then maintaining these parameters constant while varying only H_{ac} for the other data sets at different applied fields. The corresponding value for J_{c0} was roughly 10^4 \AA/cm^2 , in agreement with the previous results. A temperature dependence having $m = 2.38$ best fitted the 0.4-Oe χ'' data. Though different from that used in R - T fitting, this temperature scaling factor is once again only an approximation to a more complicated temperature dependence. Nevertheless, this form for J_c was used to fit all other χ' and χ'' data in Fig. 4(a) and Fig. 4(b), respectively. Increased deviation of the calculated curve from

the critical current is assumed independent of field. Likewise, the field range in which the $\gamma(H)$ curve decays rapidly can be approximated by a H^{-1} dependence on field, which is equivalent to the Kim model. However, as we pointed out previously,³ the H^{-1} approximation, or any H^{-n} field dependence, does not have a zero slope at $H=0$, yet our $\gamma(H)$ data points for H close to zero do exhibit this rounding.¹⁹

In Fig. 4, we show the measured ac magnetic susceptibilities for different peak-to-peak levels of applied ac magnetic field. These were measured on a Model 102 AC susceptometer, made by Phasetrack Instruments, using an ac magnetic-field frequency of 4 kHz in zero dc applied magnetic field. The amplitude of the ac field was varied from 0.04 to 4 Oe (peak-to-peak). These are compared with the calculated ac susceptibilities (solid lines), following the method of Sun *et al.*,¹⁸ except that the critical current was input as a function of both temperature and field. Sun *et al.* assume an applied ac field $H = H_{ac} \sin \omega t$, where t in this case is time, and then derive a time-dependent magnetic moment given by

the data for $2H_{ac} = 4$ Oe is likely due to the nonscaling temperature behavior. In Eq. (6), T_c was fixed at 101.29 K. This number was obtained from a quadratic fit to the values of H_{ac} plotted versus the temperature at which the peak in χ'' occurs.²⁰

IV. CONCLUSIONS

The AH model has been used to explain quantitatively magnetoresistance in our granular materials and in single crystals. The low-frequency dynamical response of granular materials via ac susceptibility can also be predicted. The microstructure is understood to give rise to the detailed shape of these dissipative phenomena (due to phase slips through weak links) and can be probed by this model in a quantitative manner.

ACKNOWLEDGMENTS

The authors would like to thank U. Landman for allowing them the use of his computing facilities and for his helpful suggestions. They would also like to thank M. Y. Chou, K. Wiesenfeld, and A. Zangwill for helpful discussions and T. T. M. Palstra for insightful comments. A. E. acknowledges support from the Alfred P. Sloan Foundation. The work of T.K.X. was supported by U.S. Department of Energy Grant No. FG05-86ER45234 (to U.L.). Theoretical simulations were performed at the Pittsburgh Supercomputer Centers supported by NSF via a grant of computer time. This work was sponsored by the U.S. Department of Energy Grant No. FG05-86ER45266.

- *To whom all correspondence should be addressed.
- ¹M. Tinkham, Phys. Rev. Lett. **61**, 1658 (1988).
- ²V. Ambegaokar and B. I. Halperin, Phys. Rev. Lett. **22**, 1364 (1969).
- ³A. C. Wright, K. Zhang, and A. Erbil, Phys. Rev. B **44**, 863 (1991).
- ⁴M. Tinkham and C. J. Lobb, in *Solid State Physics*, edited by H. Ehrenreich and D. Turnbull (Academic, New York, 1989), Vol. 42, p. 91.
- ⁵C. S. Owen and D. J. Scalapino, Phys. Rev. **164**, 538 (1967).
- ⁶R. L. Peterson and J. W. Ekin, Phys. Rev. B **37**, 9848 (1988).
- ⁷J. S. Satchell, R. G. Humphreys, N. G. Chew, J. A. Edwards, and M. J. Kane, Nature **334**, 331 (1988).
- ⁸I. K. Yanson, Zh. Eksp. Teor. Fiz. **58**, 1497 (1970) [Sov. Phys. JETP **31**, 800 (1970)].
- ⁹(a) F. Falo, A. R. Bishop, and P. S. Lomdahl, Phys. Rev. B **41**, 10983 (1990); (b) K. H. Lee, T. K. Xia, and D. Stroud, in *Physical Properties of Granular Matter*, edited by P. Sheng, G. D. Cody, and T. Geballe (Materials Research Society, Pittsburgh, 1990); T. K. Xia, Ph.D. thesis, The Ohio State University, 1990 (unpublished); (c) J. S. Chung, K. H. Lee, and D. Stroud, Phys. Rev. B **40**, 6570 (1989).
- ¹⁰M. A. Dubson, S. T. Herbert, J. J. Calabrese, D. C. Harris, B. R. Patton, and J. C. Garland, Phys. Rev. Lett. **60**, 1061 (1988).
- ¹¹T. T. M. Palstra, B. Batlogg, R. B. van Dover, L. F. Schneemeyer, and J. V. Waszczak, Phys. Rev. B **41**, 6621 (1990).
- ¹²H. Aoki, Y. Asada, T. Hatano, A. Matsushita, T. Matsumoto, and K. Ogawa, Jpn. J. Appl. Phys. **26**, L711 (1987).
- ¹³D. Shi, M. S. Boley, U. Welp, J. G. Chen, and Y. Liao, Phys. Rev. B **40**, 5255 (1989).
- ¹⁴T. T. M. Palstra, B. Batlogg, L. F. Schneemeyer, and J. V. Waszczak, Phys. Rev. Lett. **61**, 1662 (1988).
- ¹⁵T. Yamada, K. Kinoshita, A. Matsuda, T. Watanabe, and Y. Asano, Jpn. J. Appl. Phys. **26**, L633 (1987); Y. Koike, T. Nakanomyo, T. Hanaguri, T. Nomoto, and T. Fukase, *ibid.* **26**, L2069 (1987); T. Tamegai, A. Watanabe, I. Oguro, and Y. Iye, *ibid.* **26**, L1304 (1987).
- ¹⁶An explicit temperature dependence of the critical current must still be assumed, or empirically determined and input nonanalytically, as in Ref. 18.
- ¹⁷K.-H. Muller, Physica C **159**, 717 (1989).
- ¹⁸J. Z. Sun, M. J. Scharen, L. C. Bourne, and J. R. Schrieffer, Phys. Rev. B **44**, 5275 (1991).
- ¹⁹However, we find that the calculation of $\chi(T)$ is not very sensitive to the exact analytic form assumed for the field dependence of the critical current.
- ²⁰Characterization of High T_c Superconductors using the Model 102 AC Susceptometer, by Phasetrack Instruments, Santa Clara, CA, 1989 (unpublished).